Optimal Path for Global Land Use under Climate Change Uncertainty

J. Steinbuks, The World Bank
Y. Cai, Hoover Institution, Stanford University
J.W. Elliott, Computation Institute, University of Chicago
T.W. Hertel, Department of Agricultural Economics, Purdue University
and
K.L. Judd, Hoover Institution, Stanford University

Selected Paper prepared for presentation at the Agricultural & Applied Economics Association's 2013 AAEA & CAES Joint Annual Meeting, Washington, DC, August 4-6, 2013

Optimal Path for Global Land Use under Climate Change Uncertainty

J. Steinbuks, The World Bank
Y. Cai, Hoover Institution, Stanford University
J.W. Elliott, Computation Institute, University of Chicago
T.W. Hertel, Department of Agricultural Economics, Purdue University
and
K.L. Judd, Hoover Institution, Stanford University*

PRELIMINARY AND INCOMPLETE
PLEASE DO NOT CITE

June 8, 2013

Abstract

This study seeks assess how the uncertainties associated with the underlying biophysical processes influence the optimal profile of land use over the next century, in light of potential irreversibility in these decisions. Our analysis is based on a dynamic stochastic model of global land use, and employs 3 modeling scenarios constructed using global crop simulation and climate models. The results of the deterministic model show that climate impacts appear to have mixed effects on yields - higher temperatures hurt food production but this effect is partially offset by greater CO_2 fertilization effect. Declining food crop yields result in relatively small expansion of cropland and accumulated GHG emissions from land use change. We then contrast this optimal path to that obtained when the uncertainty is not ignored, thereby demonstrating significance of factoring uncertainty in the optimization stage.

JEL: C61, Q15, Q23, Q26, Q40, Q54

Keywords: climate change, crop yields, dynamic stochastic models, global land use, uncertainty

*Authors appreciate financial support from the National Science Foundation, grant 0951576 "DMUU: Center for Robust Decision Making on Climate and Energy Policy".

1 Introduction

The allocation of the world's land resources over the course of the next century has become a pressing research question. Continuing population increases, improving, land-intensive diets amongst the poorest populations in the world, increasing production of biofuels and rapid urbanization in developing countries are all competing for land even as the world looks to land resources to supply more environmental services. The latter include biodiversity and natural lands, as well as forests and grasslands devoted to carbon sequestration. And all of this is taking place in the context of faster than expected climate change which is altering the biophysical environment for land-related activities. This combination of intense competition for land, coupled with highly uncertain future productivities and valuations of environmental services, gives rise to a significant problem of decision-making under uncertainty. The issue is compounded by the inherent irreversibility of many land use decisions.

Change impacts on yields and available area in agriculture and forestry sectors have received significant attention in the agronomic, biophysical, and economic literatures (Parry et al. 2004, Lobell and Field 2007, Reilly et al. 2007, Lobell and Burke 2008, Gumpenberger et al. 2010, Hertel, Burke and Lobell 2010, Lobell et al. 2011). The economic analysis of this issue is primarily based on large-scale computational models, which are 'backward looking' in their recursive-dynamic structure, and therefore limited ability to address important intertemporal policy issues such as e.g. inter-temporal allocation of GHG emission flows from land-use through abatement policies, efficiency implications of carbon taxes and caps, and endogenous depletion of non-renewable land resources. None of these studies explicitly incorporates climate change uncertainty into the determination of the optimal path of global land use. To the extent that uncertainty is dealt with, this is only through sensitivity analysis.

In this study, we seek to assess how the uncertainties associated with the underlying biophysical processes influence the optimal profile of land use over the next century, in light of potential irreversibility in these decisions. Our analysis is based on stochastic extension of FABLE, an integrated model of global land use, which brings together distinct strands of economic, agronomic, and biophysical literature and incorporates key drivers affecting global land-use.

The model we develop is a long-run dynamic, forward-looking, stochastic partial equilibrium framework in which the societal objective function being maximized places value on food production, liquid fuels (including biofuels), timber production, forest carbon and biodiversity. A non-homothetic AIDADS utility function represents model preferences, and, as society becomes wealthier, places greater value on eco-system services, and smaller value on additional consumption of food, energy and timber products. Given the importance of land-based emissions to any GHG mitigation strategy, as well as the potential impacts of climate change itself on the productivity of land in agriculture, forestry and ecosystem services, we aim to identify the optimal allocation of the world's land resources, over the course of the next century, in the face of alternative GHG constraints. The forestry sector is characterized by multiple forest

vintages, which add considerable computational complexity in the context of this dynamic stochastic analysis.

The model is solved over the period 2005-2204, with an emphasis on the first century. The model baseline accurately reflects developments in global land use over the 10 years that have already transpired, while also incorporating projections of population, income and demand growth from a variety of international agencies. We identify the optimal allocation of the world's land resources, over the course of the next century, in the face of variability in agricultural productivity as driven by climate change. Our comprehensive estimates of climate impacts on agricultural yields are based on the Decision Support System for Agrotechnology Transfer (DSSAT) crop simulation models for four major crops, run globally on a 0.5 degree grid and weighted by agricultural output under different GHG forcing scenarios using outputs from five different global climate models.

We first show the results of the perfect foresight model, treating uncertainty only through sensitivity analysis. Climate impacts appear to have mixed effects on yields - higher temperatures hurt food production but this effect is partially offset by greater CO_2 fertilization effect. Declining food crop yields result in greater requirements for cropland and fertilizers to produce agricultural output used in production of food services. However, the expansion of cropland is relatively small. Accumulated GHG emissions increase modestly relative to the baseline scenario as GHG emissions from the use of fertilizers increase and forest sequestration declines. Consumption of processed food services declines significantly. Declining food crop yields also depress production of first generation biofuels, whereas the production of second generation biofuels the share of biofuels in liquid fuel consumption remains practically unchanged.

We then contrast this optimal path to that obtained when the uncertainty is not ignored, thereby demonstrating the implications of factoring this in at the optimization stage.

2 Model Outline

The analysis used here employs FABLE (Forest, Agriculture, and Biofuels in a Land use model with Environmental services), a dynamic optimization model for the world's land resources over the next century. This model brings together recent strands of agronomic, economic, and biophysical literature into a single, intertemporally consistent, analytical framework, at global scale. The model solves for the dynamic paths of alternative land uses, which together maximize global economic welfare, subject to a constraint on global GHG emissions. The key model equations are described below, with complete information offered in model's technical documentation (Steinbuks and Hertel 2012).

FABLE is a deterministic, discrete dynamic, finite horizon partial equilibrium model. Income, population, wages, oil prices, total factor productivity, and other variable input prices are assumed to be exogenous. The model focuses on the optimal allocation of scarce land across competing uses across time.

There are two natural resources in the model: land and fossil fuels. The supply price of fossil fuels is predetermined, and is expected to rise over time. The supply of land is fixed and faces competing uses that are determined endogenously by the model.

We analyze eight sectors producing intermediate and final goods and services. The agrochemical sector converts fossil fuels into fertilizers that are used to boost yields in the agricultural sector. The agricultural sector combines cropland and fertilizers to produce intermediate outputs (food crops and cellulosic feed stocks) that can be used to produce food or biofuels. The food processing sector converts food crops into food products that are used to meet the global food demand. The biofuels sector converts food crops and cellulosic feedstocks into liquid fuels, which substitute imperfectly for petroleum products in final demand. The energy sector combines petroleum products with the biofuels, and the resulting mix is further combusted to satisfy the demand for energy services. The forestry sector produces an intermediate product, which is further used in timber processing. The timber processing sector converts output from the forestry sector into a final timber product, which satisfies commercial demands for lumber and other articles of wood. The ecosystem services sector provides a public good to society in the form of ecosystem services. The production of other goods and services are predetermined.

The societal objective function being maximized places value on processed food, energy services, timber products, and eco-system services. Emissions of greenhouse gases (GHGs) are central to the problem at hand. These are currently treated as a time-varying constraint on the flow of GHGs (emissions target). As the model focuses on the representative agent's behavior, the resource endowments and consumption products are expressed in per-capita terms. Full model's structure, equations, variables, and parameters are summarized in model's technical documentation (Steinbuks and Hertel 2012).

2.1 Resource Use

2.1.1 Land

The total land endowment in the model, $\overline{L}$, is fixed. The land in the economy comprises of natural forest lands - which are in an undisturbed state (e.g., parts of the Amazon), L_t^N, and managed commercial lands, L_t^M. The land endowment constraint is

$$\overline{L} = L_t^N + L_t^M. \tag{1}$$

We assume that the natural land consists of two types. Institutionally protected land, L^R, includes natural parks, biodiversity reserves and other types of protected forests. This land is used to produce ecosystem services for society, and cannot be converted to commercial land. Unmanaged natural land, L^U, can be accessed and either converted to commercial land (deforested) or to protected land. Once the natural land is deforested, its potential to yield ecosystem services is interrupted and cannot be restored within the (single century) time frame of the analysis. Thus, the conversion of natural lands for commercial use

is an irreversible decision.[1] Equations describing allocation of commercial land across time and different uses are as follows, where lower case variables describe flows and upper cases correspond to stocks:

$$L_t^N = L_t^U + L_t^R. \tag{2}$$

$$L_{t+1}^U = L_t^U - \Delta L_t^U - \Delta L_t^R,\ L_0^U > 0, \tag{3}$$

and

$$L_{t+1}^R = L_t^R + \Delta L_t^R,\ L_0^R > 0, \tag{4}$$

Equation (2) shows that the total endowment of natural land is a sum of the hectares of reserved and non-reserved natural land. Equation (3) shows that at each period of time the area of unmanaged natural land with initial stock, L_0^U, declines by the amounts allocated for conversion to commercial and protected land, ΔL_t^U and ΔL_t^R, where Δ operator denotes a change in variables L_t^U and L_t^R. Equation (4) shows that at each period of time, the total area of reserved land with initial stock of L_0^R increases by the amount of newly protected land, ΔL_t^R.

Accessing the natural lands comes at cost, c_t^U, associated with building roads and other infrastructure (Golub et al. 2009). In addition, converting natural land to reserved land entails additional costs, c_t^R, associated with passing legislation to create new natural parks. We assume that these costs are continuous, monotonically increasing, and strictly convex functions of the share of natural land previously accessed. There are no additional costs of natural land conversion to commercial land, as these costs are offset by the revenues from deforestation.

Commercial lands are used in either the agriculture or forestry sectors (we ignore residential, retail, and industrial uses of land in this partial equilibrium model of agriculture and forestry). Equations describing allocation of commercial land across time and between agriculture and forestry are:

$$L_t^M = L_t^A + L_t^C. \tag{5}$$

and

$$L_{t+1}^M = L_t^M + \Delta L_t^U,\ L_0^M > 0. \tag{6}$$

Equation (5) shows that total endowment of commercial land, L^M, is a sum of the hectares of commercial land dedicated to agriculture, L^A, and managed forest, L^C, respectively. Equation (6) shows that at each period of time, the total area of commercial land with initial stock of L_0^M increases by the amount of converted unmanaged natural land, ΔL^U.

[1] This point requires additional clarification. The biophysical and ecological literature suggests that restoration of forest structure and plant species takes at least 30–40 years and usually many more decades (Chazdon 2008), costs several to ten thousands dollars per hectare (Nesshöver et al. 2009), and is only partially successful in achieving reference conditions (Benayas et al. 2009). Modeling restoration of biodiversity under these assumptions introduces greater computational complexity without making significant changes relative to findings presented in this study.

2.1.2 Fossil Fuels

The fossil fuels, x, have two competing uses in our partial equilibrium model of land-use. A fraction of fossil fuels, x^n, is converted to fertilizers that are further used in the agricultural sector. The remaining amount of fossil fuels, x^e, is combusted to satisfy the demand for energy services. The total supply of fossil fuels is thus given by

$$x_t = x_t^n + x_t^e. \tag{7}$$

The cost of fossil fuels, c_t^x, is pre-determined, and reflects the expenditures on fossil fuels' extraction, transportation and distribution, as well the costs associated with GHG emissions control (e.g. carbon prices) in the non-land-based economy.

2.2 Agrochemical Sector

The agrochemical sector consumes an amount of fossil fuels, denoted by x^n, and converts them into fertilizers that are further used in the agricultural sector. The production of fertilizers, n, is a simple engineering process that can be described by a linear production function:

$$n_t = \theta^n x_t^n, \tag{8}$$

where θ^n is the rate of conversion of fossil fuels to fertilizers. We assume that the non-energy cost of conversion of fossil fuels to fertilizers, c^ϕ, is constant and scale-invariant.

2.3 Agricultural Sector

The agricultural sector combines the agricultural land and fertilizers to deliver an agricultural products, g^i. In the model, we distinguish between two types of agricultural outputs. Food crops, g^1, can be either consumed as food, f, or converted to first generation biofuels, b^1. Cellulosic feed stocks, g^2, can only be converted to second generation biofuels, b^2. Agricultural land and fertilizers are imperfect substitutes in the production of agricultural products. The per capita output of agricultural products, g^i, is thus determined by the constant elasticity of substitution (CES) function:

$$g_t^i = \frac{\theta_t^{g,i}}{\Pi_t}\left[\alpha^g\left(L_t^{A,i}\right)^{\rho_g} + (1-\alpha^g)\left(n_t\right)^{\rho_g}\right]^{\frac{1}{\rho_g}},\ i = 1,2, \tag{9}$$

where Π_t is the predetermined population at time, and $\theta_t^{g,i}$ and α^g are, respectively, the crop technology (agricultural yield) index and the value share of land in production of agricultural product i at the benchmark time 0, and $L_t^{A,i}$ are hectares of agricultural land allocated for food crops and cellulosic feed stocks. The parameter $\rho_g = \frac{\sigma_g - 1}{\sigma_g}$ is a CES function parameter proportional to the elasticity of substitution of agricultural land for fertilizers, σ^g. The production of

agricultural output is also subject to non-land costs from use of fertilizers and other production factors (such as e.g. labor or capital), c^g, the prices of which are predetermined in our partial equilibrium model.

2.4 Food Processing Sector

The food processing sector converts an amount of food crops, g^1, into food products and services, f, that are further consumed in final demand. The purpose of this sector in the model is to capture the efficiency gains from technology improvements in food production, which result in lower requirements for agricultural inputs in final demand.[2] The conversion process is represented by the following production function:

$$f_t = \theta_t^f g_t^1, \tag{10}$$

where θ_t^f is the total factor productivity (TFP) of the food processing sector, which captures the technological progress in both direct transformation of agricultural product into edible food, and the storage, transportation, and distribution of processed food. We assume that the food processing costs per ton of food products, c^f, are exogenous and scale-invariant.

2.5 Biofuels Sector

The biofuels sector consumes the remaining amount of food crops to produce first generation biofuels, b^1. We assume that a ton of food crops, g^1, can be converted to $\theta^{b,1}$ tons of oil equivalent ($toe's$) of first generation biofuels. The output of first generation biofuels is thus given by

$$b_t^1 = \theta^{b,1}\left(g_t^1 - \frac{f_t}{\theta^f}\right). \tag{11}$$

The biofuels sector also converts cellulosic feedstocks, g^2, into second generation biofuels, b^2. Second generation biofuels are a new technology, which is expected to take over a market gradually. The temporal path of the share of the market controlled by this new technology is expected to follow some type of S-shaped function (Geroski 2000). There are many reasons cited for such gradual penetration, including capital adjustment costs, scarcity of specialized engineering resources and the necessary equipment to install new capacity, and slow regulatory approval processes. In this study, the approach for representing the penetration process is based on McFarland et al. (2004), and is similar to that used in MIT-EPPA integrated assessment model (Paltsev et al. 2005). We explicitly introduce in the production function an additional fixed factor specific to the new technology, ϕ, whose endowment in the economy limited. As

[2]For example, technological innovation in food conservation results in fewer losses from spoilage, and, correspondingly, lower amounts of processed food needed to satisfy the commercial demand for food. Correspondingly, input requirements for agricultural product also decrease.

technology penetrates the market the share of technology fixed factor in the production function declines with the rate of factor-specific technological progress, θ_t^{ϕ} (van Meijl and van Tongeren 1999). Under this assumptions the production of second generation biofuels, b^2, is determined by the following CES function

$$b_t^2 = \theta^{b,2} \left[\left(\alpha^b\right)^{\theta_t^{\phi}} (\phi)^{\rho_b} + \left(1-\alpha^b\right) \left(g_t^2\right)^{\rho_b} \right]^{\frac{1}{\rho b}}, \tag{12}$$

where where $\theta_t^{b,2}$ and α^b are, respectively, the technology parameter and the value share of fixed factor in production of second generation biofuels at the benchmark time 0. The parameter $\rho_b = \frac{\sigma_b - 1}{\sigma_b}$ is a CES function parameter proportional to the elasticity of substitution of technology fixed factor for cellulosic feed stocks, σ^b. The agricultural products' conversion to renewable fuel incurs additional non-food processing costs, $c^{b,i}$. We assume these costs are constant and scale-invariant.[3]

2.6 Energy Sector

The energy sector consumes petroleum products, x^e, and first and second generation biofuels, b^i. First generation biofuels (e.g., corn or sugarcane ethanol) blend with petroleum products in different proportions[4], and the resulting mix further combusted to satisfy the demand for energy services. We assume that first-generation biofuels and petroleum products are imperfect substitutes. Second generation biofuels (e.g., cellulosic biomass-to-liquid diesel obtained through Fischer-Tropsch gasification) offer a full 'drop-in' fuel alternative. We therefore assume that petroleum products and second generation biofuels are perfect substitutes. Under these assumptions the production of energy services per capita, e_t, is given by CES function:

$$e_t = \theta_t^e \left(\alpha^e \left(b_t^1\right)^{\rho_e} + (1-\alpha^e) \left(\frac{x_t^e}{\Pi_t} + b_t^2 \right)^{\rho_e} \right)^{\frac{1}{\rho e}}, \tag{13}$$

where the parameter θ^e describes the efficiency of energy production, (i.e., the amount of energy services provided by one *toe* of the energy fuel, Sorrell and Dimitropoulos 2008, p. 639), α^e is the value share of first-generation biofuels in energy production at the benchmark time 0, and $\rho_e = \frac{\sigma_e - 1}{\sigma_e}$ is a CES function parameter proportional to the elasticity of substitution of petroleum products for first generation biofuels, σ_e.

[3] With introduction of second generation biofuels one would expect these costs to decline, and biofuels conversion rate to increase as the biofuels' production technology improves. We show the model sensitivity to changes in these parameters in model's technical documentation (Steinbuks and Hertel 2012).

[4] Blends of E10 or less are used in more than twenty countries around the world, led by the United States, where ethanol represented 10% percent of the U.S. gasoline fuel supply in 2011. Blends from E20 to E25 have been used in Brazil since the late 1970s. E85 is commonly used in the U.S. and Europe for flexible-fuel vehicles. Hydrous ethanol or E100 is used in Brazilian neat ethanol vehicles and flex-fuel light vehicles and in hydrous E15 called hE15 for modern petrol cars in Netherlands.

The total non-land cost of energy is a sum of the costs of fossil fuels and biofuels net of land-use costs:

$$c_t^e = \sum_i c^{b,i} + c_t^x,\ i = 1, 2. \tag{14}$$

2.7 Forestry Sector

The forestry sector is characterized by v vintages of trees. At the end of period t each hectare of managed forest land, $L_{v,t}^C$, has an average density of tree vintage age v, with the initial allocation given and denoted by $L_{v,0}^C$. Each period of time the managed forest land can be either planted, harvested or simply left to mature. The newly planted trees occupy $\Delta L^{C,P}$ hectares of land, and reach the average age of the first tree vintage next period. The harvested area occupies $\Delta L_v^{C,H}$ hectares of forest land. If the managed forest land is harvested, it yields θ_v^w tons of forest product (raw timber), w_v, where θ_v^w is the merchantable timber yield function, which is monotonically increasing in the average tree density of age v. Forest land becomes eligible for harvest when planted trees reach a minimum age for merchantable timber, $\overline{v}$. Managed forest areas with the average density of oldest trees $v_{\max}$ have the highest yield of $\theta_{v_{\max}}^w$. They do not grow further and stay until harvested.

We assume that the average harvesting costs per ton of forest product, are invariant to scale and are the same across all managed forest areas of different age. With continuous growth up to vintage $v_{\max}$, the average long-run cost of harvesting per hectare of managed forest land, c^w, is therefore a declining function of timber output. Harvest of managed forests and conversion of harvested forest land to agricultural land is subject to additional near term adjustment costs. The average planting costs per hectare of newly forest planted, c^p, are invariant to scale and are the same across all vintages.

The following equations describe the forestry sector:

$$L_t^C = \sum_{v=1}^{v_{\max}} L_{v,t}^C, \tag{15}$$

$$L_{v+1,t+1}^C = L_{v,t}^C - \Delta L_{v,t}^{C,H},\ v < v_{\max} - 1 \tag{16}$$

$$L_{v_{\max},t+1}^C = L_{v_{\max},t}^C - \Delta L_{v_{\max},t}^{C,H} + L_{v_{\max}-1,t}^C - \Delta L_{v_{\max}-1,t}^{C,H} \tag{17}$$

$$L_{1,t+1}^C = \Delta L_t^{C,P}, \tag{18}$$

and

$$w_t = \sum_{v=1}^{v_{\max}} \frac{\theta_{v,t}^w}{\Pi_t} \Delta L_{v,t}^{C,H}, \tag{19}$$

Equation (15) describes the composition of managed forest area across forest vintages. Equation (16) illustrates the harvesting dynamics of forest areas with the average ages v and $v_{\max}$. Equation (18) shows the transition from planted area, $\Delta L_t^{C,P}$, to new forest vintage area. Equation (19) describes the output of forest product per capita from harvested forest areas of average tree age v.

2.8 Timber Processing Sector

The timber processing sector converts harvested forest product, w, into processed timber products, s, that are further consumed in final demand. Similar to food processing, the purpose of this sector in the model is to capture the efficiency gains from technology improvements in timber production, which result in lower requirements for forest products in final demand.[5] The conversion process is represented by a linear production function:

$$s_t = \theta_t^s w_t, \tag{20}$$

where θ^s is the TFP of the timber processing sector, which captures the technological progress in both direct transformation of forest product into processed timber, and the quality improvements and durability of timber products. We assume that the timber processing costs per ton of food products, c^s, are exogenous and scale-invariant.

2.9 Ecosystem Services Sector

The ecosystem services sector combines different types of land to produce terrestrial ecosystem services. It is well known in both economic and ecological literatures that ecosystem services are difficult to define, and it is even more difficult to characterize their production process (National Research Council 2005). This stems in part from the fact that there is a significant heterogeneity in ecosystem services (Costanza et al. 1997, Daily 1997), which include physical products (e.g., subsistence food and lumber) environmental services (e.g., pollination and nutrition cycling), and non-use goods which are valued purely for their continued existence (e.g., some unobserved biodiversity). In many cases the lack of markets and market prices impedes the translation from quantities of ecosystem goods and services to their production values, and requires the application of non-market and experimental valuation techniques (Bateman et al. 2011). And there are significant differences in definitions and modeling approaches in the economic and ecological literatures, which the National Research Council 2005, p.3 refers to "the greatest challenge for successful valuation of ecosystem services". While addressing these limitations is beyond the scope of this study, given their important role in the evolution of the long run demand for land, we incorporate ecosystem services, albeit in a stylized fashion, into the global land use model determining the optimal dynamic path of land-use in the coming century.

We assume that the per capita output for ecosystem services, r_t, is given by the following CES function of different land inputs:

$$r_t = \frac{\theta^r}{\Pi_t}\left[\alpha^{A,r}\left(L^A\right)^{\rho_r} + \alpha^{C,r}\left(L^C\right)^{\rho_r} + \left(1-\alpha^{A,r}-\alpha^{C,r}\right)\left(L^U + \theta_t^R L^R\right)^{\rho_r}\right]^{\frac{1}{\rho r}}. \tag{21}$$

[5] For example, technological innovation in durability of timber products results in their less frequent replacement. Therefore lower amounts of forest product are needed to satisfy the commercial demand for timber products.

where the parameter θ^r describes the production "technology" of ecosystem services[6]. The parameters $\alpha^{A,r}$, $\alpha^{C,r}$, and $1-\alpha^{A,r}-\alpha^{C,r}$ are the value shares of agricultural, managed, and natural forest lands in production of ecosystem services at the benchmark time 0. The parameter $\rho_r = \frac{\sigma_r - 1}{\sigma_r}$ is a CES function parameter proportional to the elasticity of substitution of different types of land in production of ecosystem services, σ_e. By characterizing the production process of ecosystem services using equation (21) we assume that agricultural, managed forest, and natural lands substitute imperfectly in production of ecosystem services. Unmanaged and protected natural land produce the same ecosystem services (Costanza et al. 1997). However, protected forest lands are more efficient in delivering many ecosystem services, as they have e.g., better management for reducing degradation of biodiversity, and better infrastructure for providing eco-tourism and recreation services (Hocking et al. 2000).

We assume that non-land cost of producing ecosystem services is zero for agricultural and managed forest land, as production of ecosystem services is not their primary function. This cost is also zero for unmanaged natural lands. As regards protected natural lands, we assume that average non-land cost of producing ecosystem services (e.g., maintenance and infrastructure expenditures) per hectare of reserved natural land, c^r, is exogenous and scale-invariant.

2.10 Other Goods and Services

The production of other goods and services per capita, o_t, in this model is predetermined. The reason we include it in this partial equilibrium model is to complete the demand system (described in a section below), which determines welfare. As the supply of other goods and services is predetermined, we assume that they grow at the overall rate of TFP growth, which is equal to the world economy's TFP growth rate[7]. Because the production of other goods and services does not draw on the land resource, we assume without loss of generality that their cost of production is zero.

2.11 GHG Emissions

The GHG emissions flows, z_t, in the model result from a number of sources: (a) combustion of petroleum products, (b) the conversion of unmanaged and managed forests to agricultural land (deforestation), (c) non-CO_2 emissions from use of fertilizers in agricultural production, and (d) net GHG sequestration through forest sinks (which includes the GHG emissions from harvesting forests). We differentiate between the emissions resulting from combustion of petroleum products and the emissions resulting from land-use, z^L, because the price path

[6] We put the term "technology" in quotation terms because, as discussed above, characterizing "true" production process of ecosystem services is beyond the scope of the paper. Here we use the term "technology" as a scalar that maps ecological assets to ecosystem services in reference period 0.

[7] The economy's output has a small fraction of endogenously determined output from land-use. We ignore this complication in this partial-equilibrium model.

for fossil fuels is pre-determined, whereas the other sources of GHG emissions are endogenous.

We assume that GHG emissions are linearly related to the use of fossil fuels, and the allocations of commercial lands. A ton of oil equivalent *(toe)* of fossil fuel combusted emits μ^x tons of CO_2 equivalent (tCO_2e). A ton of fertilizer applied to agricultural land emits μ^n tCO_2e.

GHG's can also be reduced by carbon forest sequestration.[8] A hectare of forest vintage v sequesters μ_v^w tCO_2e. Young forest vintages grow quickly and sequester carbon at a rapid rate. Older vintages grow slowly and eventually cease to sequester carbon. As the unmanaged forest land (both reserved and non-reserved) comprises mainly the older tree vintages, its potential to sequester additional GHGs is small, and may be ignored. However, the potential for GHG releases when these trees are cut down and burned or left as slash (Fearnside 2000, Houghton 2003) is large. The conversion of natural forest land to commercial land entails emissions of μ^L tCO_2e per hectare of land deforested. Harvesting managed forests results in emissions of $(1-\varphi)\mu_v^h$ tCO_2e per hectare of land harvested, where μ_v^h is the carbon stock associated with harvested tree vintage v, and φ is the share of permanently stored carbon in harvested forest products. We ignore the annual sequestration of carbon by agricultural product, as those crops are harvested and subsequently consumed in the form of food or bioenergy.

Based on the above, the equations describing net GHG flows in the economy are

$$z_t = \mu^x x_t^e + z_t^L, \tag{22}$$

and

$$z_t = \mu^L \Delta L_t^U + \mu^n x_t^n + (1-\varphi)\sum_{v=1}^{v_{\max}} \mu_v^h \Delta L_{v,t}^{C,H} - \sum_{v=1}^{v_{\max}} \mu_v^w L_{v,t}^C. \tag{23}$$

Equation (22) describes the composition of GHG emissions flows. Equation (23) shows net GHG emissions from deforestation, agricultural production, and forest sequestration.

Finally, we consider institutional control of GHG emissions' flows (e.g. through the Kyoto Protocol), which foresees their gradual reduction and the stabilization of atmospheric carbon stocks. Specifically, we assume that at any point of time net GHG emissions from deforestation, application of fertilizers, and forest sequestration cannot exceed the emissions' quota, $\overline{z}^L$. We do not impose the emissions' constraints on GHG emissions from fossil fuels' combustion because they are exogenously determined. Rather we assume that emissions control instruments are reflected in exogenous fossil fuels' prices, which affect the demand for fossil fuels. Finally, because biofuels provide a renewable alternative to fossil fuels, we credit the emissions' quota, $\overline{z}^L$,by the fraction of fossil fuels' emissions

[8] GHG emissions flows are also sequestered by atmospheric and ocean sinks. We ignore this complication as our model does not provide comprehensive accounting of all GHG emissions flows, and focuses on understanding emissions from land use and related sectors.

displaced by the biofuels.[9] The resulting relationships for emissions control are

$$z_t^L \leq \overline{z}_t^L = \theta_t^z \left(z_t^L - \left(1 - \frac{\mu^{b,i}}{\mu^x} \right) b_t^i \right), i = 1, 2. \tag{24}$$

where global warming intensity, θ_t^z is a function determining the evolution of the GHG emissions' quota over time, and $\mu^{b,1}$ and $\mu^{b,2}$ are non-land-use emissions of first and second generation biofuels' production. Equation (24) describes the constraint on non-fossil fuel emissions in the atmosphere, and shows how this constraint is derived.

2.12 Preferences

The representative agent's utility, U, is derived from the consumption of food products, energy services, timber products, ecosystem services and other goods and services. The specific functional form for the utility function in this study is based on implicitly directive additive preferences, AIDADS (Rimmer and Powell 1996). Our choice of the utility function based on AIDADS preferences is motivated by its several important advantages over other functional forms underpinning standard models of consumer demand.[10] First, similar to the well-known AIDS demand system (Deaton and Muellbauer 1980) the AIDADS model is flexible in its treatment of Engel effects, i.e. the model "allows the MBS' (Marginal Budget Shares) to vary as a function of total real expenditures" Rimmer and Powell (1996, p. 1614). Second, the AIDADS has global regularity properties, in contrast to the local properties of AIDS[11]. This is essential for solution of the model over a wide range of quantities. A number of studies (Cranfield et al. 2003, Yu et al. 2004) demonstrated that AIDADS outperforms other popular models of consumer demand in projecting global food demand, which makes it especially well-suited for the economic modeling of land-use.

The utility function for the AIDADS system is the implicitly directly additive function (Hanoch 1975):

$$\sum_{q=f,e,w,r,o} F\left(\overrightarrow{q}, u \right) = 1, \tag{25}$$

where $\overrightarrow{q} = \{f, e, w, r, o\}$ is the consumption bundle, u is the utility level obtained from the consumption of goods or services q, and $F(q, u)$ is a twice-diffirentiable monotonic function that is strictly quasi-concave in $\overrightarrow{q}$. Based on

[9] This doesn't necessarily mean that biofuels are 'greener' than fossil fuels. That will depend on the emissions associated with agricultural production and natural land conversion.

[10] The most popular demand systems estimated in recent applied work are the Homothetic Cobb-Douglas System (HCD), the Linear Expenditure System (LES), the Constant Difference of Elasticities Demand System (CDE), and the Almost Ideal Demand System (AIDS).

[11] One of well-known limitations of the AIDS system is that its budget shares fall outside $[0, 1]$ interval. This frequently occurs when AIDS is applied to model the demand for staple food when income growth is large (Yu et al. 2004, p. 102).

Rimmer and Powell (1996), the functional form for $F\left(\overrightarrow{q}, u\right)$ is

$$F\left(\overrightarrow{q}, u\right) = \frac{\alpha_q + \beta_q \exp(u)}{1 + \exp(u)} \ln\left(\frac{\overrightarrow{q} - \underline{q}}{A \exp(u)}\right). \tag{26}$$

In equation (26) the parameters α_q and β_q define the varying marginal budget shares of goods and services $\underline{q}$ in the consumers' total real expenditures. The parameter $\overline{q}$ defines the subsistence level of consumption of goods and services $\overrightarrow{q}$. The functional form of $F\left(\overrightarrow{q}, u\right)$ implies that the consumption of goods and services q is always greater than their subsistence levels, $\underline{q}$. The parameter A affects the curvature of the transformation function $F\left(\overrightarrow{q}, u\right)$. The AIDADS system imposes standard non-negativity and adding-up restrictions based on the economic theory. These restrictions ensure that the consumers' marginal budget shares and minimal consumption level of goods and services $\underline{q}$ are greater or equal to zero, and the sum of marginal budget shares in total real expenditures does not exceed one.

Rimmer and Powell (1996, p. 1615) demonstrate that maximizing the utility function (25) subject to the budget identity constraint (26) yields the following system of inverse demand equations:

$$\overrightarrow{p}_q\left(\overrightarrow{q}\right) = \frac{\alpha_q + \beta_q \exp(u)}{1 + \exp(u)} \frac{y - \sum_q \overrightarrow{p}_q \overrightarrow{q}}{\overrightarrow{q} - \underline{q}}, \tag{27}$$

where $\overrightarrow{p}_q$ are "prices" - or in this case, the marginal valuation - of goods and services $\overrightarrow{q}$ and y is the economy's output per capita.

2.13 Welfare

The objective of the planner is to maximize welfare function, Ω, defined as the sum of net aggregate surplus discounted at the constant rate $\delta > 0$, and the bequest value of unmanaged and commercial forest areas.[12] Net surplus is computed by integrating the marginal valuation of each product, less the land access costs and non-land-based costs of producing each good. Thus, for agricultural output, food, and timber products, this represents non-land production costs. For energy, these are non-land biofuels costs and fossil fuel costs. For fertilizers, these are non-energy costs. For forestry, these are harvesting and planting costs. And for recreation, these are the costs of maintaining natural parks. The planner allocates commercial land for agricultural product and timber production, and the scarce fossil fuels and reserved natural forest land to solve the following

[12] We do not consider the bequest value of protected forests, as they cannot be "scrapped" in our model.

problem:

$$\max_{f,e,s,r} \Omega = \sum_{t=0}^{T-1} \delta^t \left[\sum_{q=f,e,s,r,o} \int_0^{q^*} \left(\overrightarrow{p}_q \left(\overrightarrow{q} \right) - c_q \left(\overrightarrow{q} \right) \right) d\overrightarrow{q} - c_t^U \left(\Delta L^U + \Delta L^R \right) - c_t^R - c^n n_t - c_t^g g_t - c^p \Delta L_t^{C,P} - c_t^w \right] + \delta^T \Gamma \left(L_T^U, L_T^C \right) \quad (28)$$

s.t. constraints (1)-(27), where Γ is the scrap value function.

3 Introducing Uncertainty Into Optimization Stage

An important limitation of FABLE model is that it is a deterministic model, which accounts for uncertainty only through sensitivity analysis of model parameters, and ignores its impact on agents' decisions. Developing the stochastic extension of the model is a complex problem, because of the vintage representation of the forestry sector (as described by equations 15-18), which adds considerable computational complexity in the context of a dynamic stochastic analysis. This section shows theoretical approach for incorporating uncertainty in the decision making stage of FABLE model.

We solve the stochastic problem by numerical dynamic programming algorithms. The dynamic programming formulation of the model is the following Bellman equation Bellman (1957):

$$V_t \left(L_t^N, L_t^A, L_t^R, L_t^C \right) = \max \Omega_t \left(\overrightarrow{q_t} \right) + \delta \mathbb{E} \left\{ V_{t+1} \left(L_{t+1}^N, L_{t+1}^A, L_{t+1}^R, L_{t+1}^C \right) \right\}, \quad (29)$$

for $t < T$. The terminal value function is given by computing the discounted summation of payoffs with fixed control policies over the period $[T+1, T+200]$, for each possible terminal state vector $\left(L_T^N, L_T^A, L_T^R, L_T^C \right)$.

In dynamic programming problems, when the value function is continuous, it has to be approximated. We use a finitely parameterized collection of functions to approximate a value function, $V(x) \approx \hat{V}(x; \mathbf{b})$, where x is the continuous state vector (in this study, it is the $(v_{\max} + 3)$-dimensional vector, $\left(L^N, L^A, L^R, L^C \right)$) and $\mathbf{b}$ is a vector of parameters. The functional form $\hat{V}$ may be a linear combination of polynomials, or it may represent a rational function or neural network representation, or it may be some other parameterization especially designed for the problem. After the functional form is fixed, we focus on finding the vector of parameters, $\mathbf{b}$, such that $\hat{V}(x; \mathbf{b})$ approximately satisfies the Bellman equation. Numerical DP with value function iteration can solve the Bellman equation approximately Judd (1998). Thus, the Bellman equation (29) can be rewritten in a general form:

$$V_t(x) = \max_{a \in \mathcal{D}(x,t)} \Omega_t(x, a) + \delta \mathbb{E} \left\{ V_{t+1}(x^+) \right\}, \quad s.t. \;\; x^+ = f(x, a, \omega),$$

where $V_t(x)$ is the value function at time $t \leq T$ (the terminal value function $V_T(x)$ is given), a is the action variable vector (in this study, it includes $\Delta L^U, \Delta L^R, \Delta L^{C,H}, \Delta L_t^{C,P}, \overrightarrow{q}$, etc.), x^+ is the next-stage state vector $\left(L_{t+1}^N, L_{t+1}^A, L_{t+1}^R, L_{t+1}^C\right)$, $\mathcal{D}(x,t)$ is a feasible set of a, ω is a random variable, δ is a discount factor and $\Omega_t(x,a)$ is the payoff function at time t. The following is the algorithm of parametric dynamic programming with value function iteration for finite horizon problems. Detailed discussion of numerical DP can be found in Cai (2010), Judd (1998) and Rust (2008).

Algorithm 1 Value Function Iteration for the General Dynamic Programming Model

Initialization. *Choose the approximation nodes,* $\mathbb{X}_t = \{x_{i,t} : 1 \leq i \leq N_t\}$ *for every* $t < T$*, and choose a functional form for* $\hat{V}(x; \mathbf{b})$*. Let* $\hat{V}(x; \mathbf{b}^T) = V_T(x)$*. Then for* $t = T-1, T-2, \ldots, 0$*, iterate through steps 1 and 2.*

Step 1. *Maximization step. Compute*

$$v_i = \max_{a \in \mathcal{D}(x^i,t)} \Omega_t\left(x^i, a\right) + \beta \mathbb{E}\left\{\hat{V}\left(x^+; \mathbf{b}^{t+1}\right)\right\}, \tag{30}$$

for each $x^i \in \mathbb{X}_t$*,* $1 \leq i \leq N_t$*, where* x^+ *is the next-stage state transition from* x^i*.*

Step 2. *Fitting step. Using an appropriate approximation method, compute* $\mathbf{b}^t$*, such that* $\hat{V}(x; \mathbf{b}^t)$ *approximates* $\{(x^i, v_i)$*:* $1 \leq i \leq N_t\}$ *data, i.e.,* $v_i \approx \hat{V}(x^i; \mathbf{b}^t)$ *for all* $x^i \in \mathbb{X}_t$*.*

Algorithm 1 includes three types of numerical problems. First, we need to solve a maximization problem at each node $x^i \in \mathbb{X}_t$. Second, the evaluation of the objective requires us to compute an expectation. Third, we need to efficiently take the data and compute the best fit for the new value function. The challenge is not only to use good numerical methods for each of these steps but also to choose methods that are compatible with each other and jointly lead to efficient algorithms. Our code is written in FORTRAN and uses the methods presented in Judd (1998), Cai (2010), and Cai and Judd (2010, 2012b, 2012a, 2012c, 2013) and we use NPSOL Gill et al. (1998) as the optimization solver in the maximization step. Since this is a high-dimensional problem, we use parallel dynamic programming methods presented in Cai et al. (2013) and apply them in a supercomputer.

4 Agricultural Yield Dynamics under Climate Scenarios

This section describes agricultural yields dynamics in FABLE model and quantifies their range of uncertainty under different climate scenarios. A well established fact in the agronomic literature is that yields of major food crops grow linearly, adding constant amount of gain per annum. However, recent agronomic evidence (Cassman et al. 2010) shows that yields are plateauing in some of the world's most important cereal-producing countries. Cassman (1999) suggested that average national yields plateau when they reach 70–80% of the genetic yield potential ceiling. Based on this hypothesis we assume that crop technology index, $\theta^{g,1}$ follows logistic (Verhulst) model with declining growth over time:

$$\theta_t^{g,1} = \frac{\theta_T^{g,1}\theta_0^{g,1}e^{\kappa_g t}}{\theta_T^{g,1} + \theta_0\left(e^{\kappa_g t} - 1\right)}, \tag{31}$$

where $\theta_0^{g,1}$ is the initial value of crop technology index, $\theta_T^{g,1}$ is crop yield potential, i.e., "the yield an adapted crop cultivar can achieve when crop management alleviates all abiotic and biotic stresses through optimal crop and soil management" (Evans and Fischer 1999), and κ_g is the logistic growth rate. In a comprehensive study Lobell et al. (2009) report a significant variation in the ratios of actual to potential yields for major food crops across the world, ranging from 0.16 for tropical lowland maize in Sub-Saharan Africa to 0.95 for wheat in Haryana, India. We assume the average ratio of 0.55. We calibrate the value of the logistic growth rate κ_g to match recent crop yield dynamics, and allow for yield plateau when they reach 70–80% of the potential yield, $\theta_T^{g,1}$.

The impact of climate change on food crop yields depends critically on their phenological development, which, in turn, depends on the accumulation of heat units, typically measured as growing degree days (GDDs). More rapid accumulation of GDDs as a result of the climate change speeds up phenological development, thereby shortening key growth stages, such as the grain filling stage, hence reducing potential yields (Long 1991). However, raising concentrations of CO_2 in the atmosphere results in an increase in potential yields due to the "CO_2 fertilization effect" (Long et al. 2006). Sorting out between relative importance of these effects and achieving more robustness in evaluating climate impacts on agricultural yields remains an important research question in agronomic and biophysical literatures (Cassman et al. 2010, Rosenzweig et al. 2013).

To quantify the range of uncertainty of climate change impact on potential crop yields we obtained results from runs of the Decision Support System for Agrotechnology Transfer (DSSAT) crop simulation model (Jones et al. 2003), run globally on a 0.5° grid and weighted by agricultural output of four major food crops (maize, soybeans, wheat and rice) under most optimistic (RCP2.6) and pessimistic (RCP8.5) Representative Concentration Pathways GHG forcing

Table 1: Changes in Potential Crop Yields by 2100 (t / Ha)

Model / Scenario	RCP 2.6F	RCP2.6NF	RCP 8.5F	RCP 8.5NF
GFDL-ESM2M	0,17	-0,16	0,46	-0,72
HadGEM2-ES	0,16	-0,18	-0,27	-1,30
IPSL-CM5A-LR	0,04	-0,29	-0,27	-1,30
MIROC-ESM-CHEM	-0,03	-0,34	-0,34	-1,32
NorESM1-M	0,20	-0,12	0,16	-0,92

Notes. F: Fertilization Effect; NF: No Fertilization Effect.
The results are normalized relative to $\theta_T^{g,1} = 8.8$.

scenarios (Moss et al. 2008) and alternate assumptions on CO_2 fertilization effects over the period between 1971 and 2099. To quantify temperature increases due to climate change we employ outputs for five global climate models (GCM): GFDL-ESM2M (Dunne et al. 2013), HadGEM2-ES (Collins et al. 2008), IPSL-CM5A-LR (Dufresne et al. 2012), MIROC-ESM-CHEM (Watanabe et al. 2011), and NorESM1-M (Bentsen et al. 2012). For each of the simulations we fit a linear trend, which is used to predict dynamics of agricultural yields over time.

Table 1 summarizes simulation results for four climate scenarios (RCP 2.6 and 8.5 with and without fertilization effects) in 2100, normalized relative to assumed yield potential of 8.8 t / Ha. There is a significant heterogeneity in terms of both direction and the magnitude of climate impacts on agricultural yields across global climate models when fertilization effect is considered. For the most optimistic scenario, RCP2.6 with fertilization effect (RCP2.6F), four out of five GCMs predict an increase in potential yields, whereas one model (MIROC-ESM-CHEM), predicts a very small decline in potential yield. In a scenario of rapid increases in global temperature with CO_2 fertilization effect (RCP8.5F) three out of five GCMs predict a decline in potential yields of comparable magnitude (between 0.27 and 0.34 t / Ha). Another GCM (NorESM1-M) predicts an increase in potential yields, but to a lesser extent as compared to scenario RCP2.6F. Only one climate model (GFDL-ESM2M) predicts an increase in potential yields, which is greater than in scenario RCP2.6F. These results are consistent with recent findings showing the potential for negative climate impacts on major crops at higher levels of warming (Rosenzweig et al. 2013).

The predictions of global climate models become more similar, at least in terms of impact direction, when CO_2 fertilization effects are removed. For a scenario of moderate temperature increases without fertilization effect (RCP2.6NF), all GCMs predict a moderate decline in potential yields (between 0.12 and 0.34 t / Ha). Three out of five GCMs predict a decline in potential yields of a comparable magnitude to scenario RCP8.5F. Finally, for a scenario of rapid temperature increases without fertilization effect (RCP8.5NF), all GCMs predict a larger decline in potential yields (between 0.72 and 1.32 t / Ha). These results are consistent with recent statistical evidence showing that "10 years of climate trend is equivalent to a setback of roughly 1 year of technology gains"

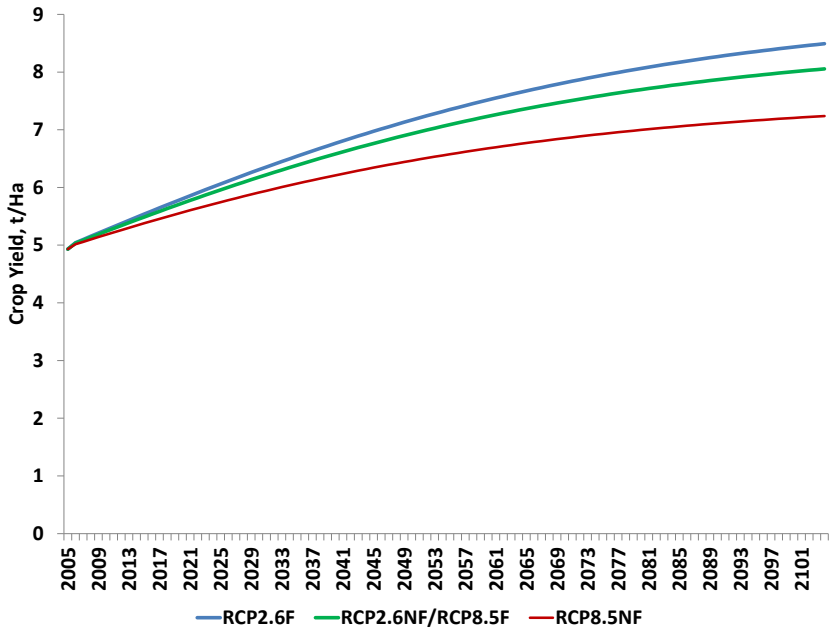

Figure 1: Crop Yield Dynamics under Different Climate Scenarios

(Lobell et al. 2011, p. 619).

Based on these results we construct 3 modeling scenarios capturing crop yield dynamics as described by equation (31) under different climate scenarios (Figure 1). The first scenario, RCP2.6F, shows yield dynamics corresponding to moderate temperature increases with CO_2 fertilization effect. The second scenario, RCP2.6NF/RCP8.5F, shows yield dynamics corresponding to either moderate temperature increases without CO_2 fertilization effect or rapid temperature increases with CO_2 fertilization effect. The third scenario, RCP8.5NF, shows yield dynamics corresponding to rapid temperature increases without CO_2 fertilization effect.

5 Results from the Perfect Foresight Model

This section describes the results of change in crop yields on the optimal path of global land use under different climate scenarios based on FABLE model simulations. We solve the model over the period 2005 - 2204, and present the results for the first 100 years to minimize the effect of terminal period conditions on our analysis.

5.1 RCP 2.6 with CO_2 Fertilization Effect (Model Baseline)

Figure 2 depicts the optimal allocation of global land-use, land based GHG emissions, consumption of goods and services that draw on land resources, and consumption of biofuels under climate scenario RCP2.6F, which we choose as the model baseline over the course of next century. Beginning with the upper left-hand panel of Figure 2, we see that, in the near term decades, area dedicated to food crops increases by 18 percent compared to 2004, reaching its maximum of 1.82 billion hectares in 2040. Managed forest area remains practically unchanged at 1.57 billion hectares. Changes in areas dedicated to biofuels feedstocks and protected natural forests remain insignificant. By mid-century, slower population growth, rising real income, agricultural yields, and improvements in food processing, storage and transportation technologies result in a decline in demand for food crops and an increase in demand for managed forests. By 2100 cropland area declines to 1.37 billion hectares, or 11 percent lower than 2004. Managed forest area increases to 1.93 billion hectares, which is 20 percent larger than 2004. Growing energy prices result in significant growth in the land area dedicated to biofuels, which reaches 0.19 billion hectares by 2100. Rising real incomes, growing demand for ecosystem services, and improvements in management of natural forest lands result in strong growth in protected natural land area, which increases sharply to 0.51 billion hectares (about 2.5 times compared to 2004) in 2100.

The upper right-hand panel in Figure 2 reports gross land based annual GHG emissions flows and their net accumulation over time.[13] Positive bars in this panel denote emissions, whereas negative bars denote GHG abatement through forest sinks and biofuels offsets. Conversion of natural forest lands is a significant driver of land-based GHG emissions in the near decades, which amounts to 3 $GtCO_2e/yr$ in 2040. By mid-century, increasing access costs of natural land combined with declining demand for commercial land, results in a sharp decline in deforestation. In 2050 GHG emissions from deforestation decrease by 63 percent compared to 2004, and amount to 1.45 $GtCO_2e/yr$. They cease entirely by mid 2060s along this optimal global path of land use. GHG emissions from application of fertilizers decline steadily as prices of natural gas increase and pressure on croplands diminishes in the face of slowing global population growth and improving crop technology. In 2100 annual flows of GHG emissions from use of fertilizers amount to 0.53 $GtCO_2e/yr$, which is 85 percent smaller than 2004. GHG emissions sequestration from managed forests does not change significantly by mid-century. In the long term the amount of sequestered GHG emissions increases with the growth in managed forest area. In 2100 sequestered GHG emissions amount to 5 $GtCO_2e/yr$, which is about 2 times larger than 2004. GHG emissions offsets from biofuels are insignificant in the near term. With the arrival of second generation biofuels technology, biofuels become a significant source of land based GHG abatement due to their

[13] As this study focuses on optimal path of land based GHG emissions, the emissions from combustion of petroleum products are not shown in Figure 2.

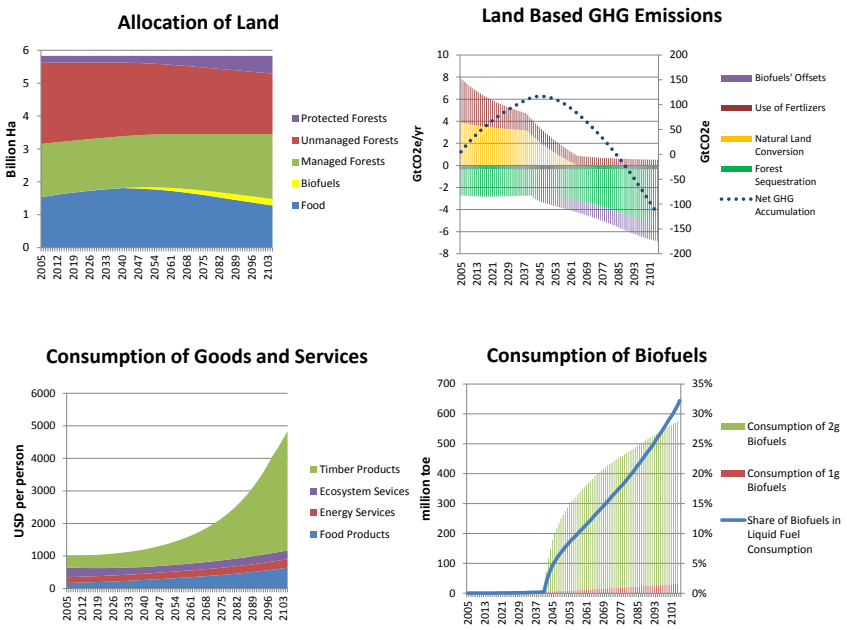

Figure 2: Model Baseline (RCP 2.6F)

low emissions intensity relative to petroleum (Dunn et al. 2011). In 2100 annual biofuels offsets account for 1.5 $GtCO_2e/yr$. Overall, accumulation of land based GHG emissions flows increases in the first part of this century, reaching its maximum of 115 $GtCO_2e$ around 2050. It then declines in the second part of the century, turning negative around 2085, and abating 90 $GtCO_2e$ by 2100. As explained above, higher oil prices, expansion of biofuels, declining deforestation, and forest growth are the main reasons for rising GHG abatement of land based sectors.

The lower left-hand panel in Figure 2 illustrates the results for per-capita consumption of goods and services that draw on land resources. The consumption of all goods and services increases in absolute terms. The growth in per capita consumption is fueled by productivity growth across the board, while population growth declines over the baseline. In 2100 the per capita consumption of services from processed food, energy, processed timber, and ecosystems is considerably higher compared to their levels in 2004. Of course, this does not translate into an equivalent increase in consumption of the bulk agriculture and timber products. Rather most of this rise in real consumption is due to efficiency gains in the processing sectors, as well as increases in the use of non-primary inputs in the production process.

The lower right-hand panel of Figure 2 describes the results for consumption

of biofuels.[14] The consumption of first generation biofuels grows slowly as oil prices and agricultural yields increase. However, along this optimal path, first generation biofuels do not become a significant source of energy consumption. In 2100 the consumption of first generation biofuels is 25 Mtoe, considerably higher than in 2004, but still small in relative terms. Second generation biofuels become competitive around 2040 and rapidly expand reaching 250 million toe in 2050, and 525 million toe in 2100. The share of biofuels in total liquid fuel consumption accounts for 7.2 percent in 2050, and for 28.5 percent in 2100. This baseline result is of comparable magnitude to findings in recent economic studies on bioenergy and land use Gurgel et al. (2007), Chakravorty et al. (2011), Popp et al. (2011).[15]

5.2 RCP 2.6 without CO_2 Fertilization Effect / RCP 8.5 with CO_2 Fertilization Effect

Figure 3 describes the results of simulations of changes in the optimal allocation of global land-use, GHG emissions, consumption of goods and services that draw on land resources, and consumption of biofuels for scenario RCP2.6NF/RCP8.5F, corresponding to decline in potential yields as a consequence of climate change. We report changes, which are incremental to the model baseline.

The upper left-hand panel in Figure 3 shows the results for changes in allocation of land use relative to the baseline scenario. Declining food crop yields result in greater requirements for cropland and fertilizers to produce agricultural output used in production of food services. However, the expansion of cropland is relatively small. Compared to the baseline scenario, the cropland area expands further by 8.5 million hectares (0.5 percent) in 2050 and by 11.5 million hectares (0.9 percent) in 2100. Managed forest area declines by 5 million hectares in 2050 and by 7 million hectares in 2100. Area dedicated to biofuels feed stocks declines by 1 million hectares in 2050, and by 2.5 million hectares in 2100. Finally, protected forest area declines by 0.5 million hectares in 2050 and by 1.5 million hectares in 2100. The modest increase in use of cropland is explained by a lower levels of total crop output than in the baseline, as well as

[14] In our baseline, biofuels expansion is driven solely by oil prices. Of course there are government mandates which have played an important role in biofuel expansion in the US and the EU, in particular. However, in the long run, we believe that the fare of biofuels will be largely determined by oil prices. In our baseline, oil prices are rising steadily such that we expect the US mandates for first generation biofuels will not be binding Meyer et al. (2011). As regards second generation biofuels, recent evidence suggests that US-RFS2 mandate for cellulosic biofuels will unlikely be met National Research Council (2011). More generally, we expect that budgetary pressures will limit the extent to which governments will be willing to subsidize biofuels in the coming decades. This leaves oil prices as the primary driver of biofuels expansion.

[15] Direct comparison of model predictions of biofuels penetration is difficult due to considerable uncertainty in variety of factors, such as, e.g., evolution of biofuels' production technologies, land access costs, yield growth rates, and energy demand projections. We show model sensitivity to these factors in counterfactual simulations in model technical documentation Steinbuks and Hertel (2012).

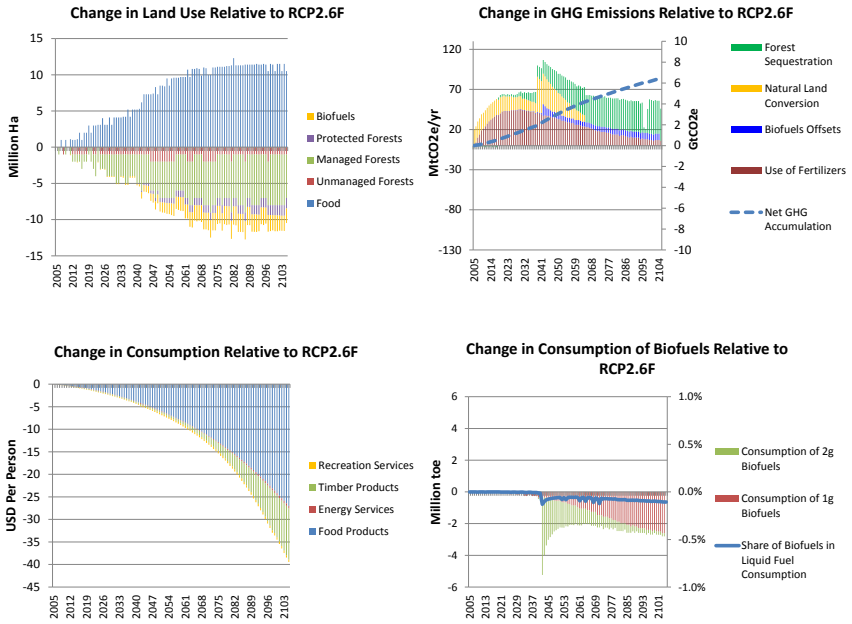

Figure 3: Scenarios RCP 2.6NF / RCP 8.5F

an increased use of fertilizers. Compared to the baseline scenario, production of food products falls by 4 percent, whereas application of fertilizers increases by 1 percent in 2100.

The upper right-hand panel in Figure 3 shows the results for changes in annual GHG emissions relative to the baseline scenario. Overall, accumulated GHG emissions change modestly relative to the baseline scenario, increasing by 6 $GtCO_2e$ in 2100. The most significant effects of declining agricultural productivity on change in GHG emissions are from greater use of fertilizers, smaller biofuels' offsets and reduced forest sequestration. Compared to the baseline scenario, the GHG emissions from fertilizers' use, reduced biofuels' offsets and forest sequestration increase by correspondingly 7, 8, and 42 $MtCO_2e/yr$ in 2100.

The lower left-hand panel in Figure 3 shows the results for changes in per-capita consumption of goods and services that draw on land resources. Compared to the baseline scenario consumption of all goods and services decreases. There is a significant decline in the consumption of processed food services. In 2100 their per capita consumption is 4 percent lower than in the baseline scenario. The reduction in consumption of services of energy, timber products, and ecosystem services is less than 1 percent.

The lower right-hand panel in Figure 3 shows the results for changes in biofuels. Declining food crop yields depress production of biofuels. In 2100 the total consumption of first generation biofuels decreases by 2.5 million toe (10 percent)

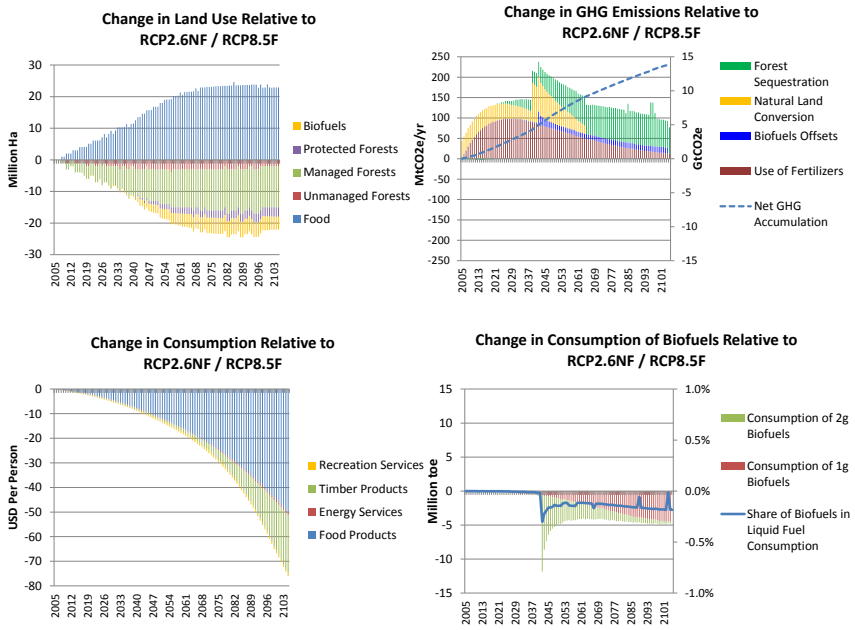

Figure 4: Scenario RCP 8.5NF

compared to the baseline scenario. The production of second generation biofuels also declines as a fraction of land dedicated to biofuels' feedstocks is substituted for cropland. However the reduction of second generation biofuels is very small and amounts to less than 1 million toe compared to the baseline scenario. As first generation biofuels account for a small share in total biofuels' consumption, the share of biofuels in liquid fuel consumption remains unchanged.

5.3 RCP 8.5 without CO_2 Fertilization Effect

Figure 4 describes the results of simulations of changes in the optimal allocation of global land-use, GHG emissions, consumption of goods and services that draw on land resources, and consumption of biofuels for scenario RCP8.5NF, corresponding to greater decline in potential yields as a consequence of rapid increase in global temperatures absent CO_2 fertilization benefits. We report changes, which are incremental to scenario RCP2.6NF/RCP8.5F. Because of same direction of climate impacts the results are very similar to previous scenario, albeit at greater magnitude.

The upper left-hand panel in Figure 4 shows the results for changes in allocation of land use relative to scenario RCP2.6NF/RCP8.5F. Declining food crop yields render further expansion of cropland. Compared to scenario RCP2.6NF /RCP8.5F, the cropland area expands further by additional 24 million hectares, whereas managed forest area declines by additional 13 million hectares in 2100.

Area dedicated to biofuels feed stocks and protected forest area decline correspondingly by additional 4 and 3 million hectares in 2100.

The upper right-hand panel in Figure 4 shows the results for changes in annual GHG emissions relative to scenario RCP2.6NF/RCP8.5F. Accumulated GHG emissions increase by additional 13 $GtCO_2e$ in 2100. The GHG emissions from fertilizers' use, reduced biofuels' offsets and forest sequestration increase further by correspondingly 15, 14, and 68 $MtCO_2e/yr$ in 2100.

The lower left-hand panel in Figure 4 shows the results for changes in per-capita consumption of goods and services that draw on land resources. Compared to scenario RCP2.6NF/RCP8.5F consumption of all goods and services decreases. Per capita consumption of services from processed food declines by additional 8 percent. The reduction in consumption of services of energy, timber products, and ecosystem services is less than 1 percent.

The lower right-hand panel in Figure 4 shows the results for changes in biofuels. In 2100 the total consumption of first generation biofuels decreases by additional 4 million toe compared to scenario RCP2.6NF/RCP8.5F. The changes in production of second generation biofuels and the share of biofuels in liquid fuel consumption are insignificant.

6 Results from the Dynamic Stochastic Model

TBC.

7 Conclusions

We seek to assess how the uncertainties associated with the underlying biophysical processes influence the optimal profile of land use over the next century, in light of potential irreversibility in these decisions. Our analysis is based on stochastic extension of FABLE, an integrated model of global land use, which brings together distinct strands of economic, agronomic, and biophysical literature and incorporates key drivers affecting global land-use.

We identify the optimal allocation of the world's land resources, over the course of the next century, in the face of variability in crop yields as driven by climate change. Our economic analysis employs 3 modeling scenarios using DSSAT crop simulation model for four major crops, run globally on a 0.5 degree grid and weighted by agricultural output under different GHG forcing scenarios using outputs from five different global climate models.

The results of the perfect foresight model show that climate impacts appear to have mixed effects on yields - higher temperatures hurt food production but this effect is partially offset by greater CO_2 fertilization effect. Declining food crop yields result in greater requirements for cropland and fertilizers to produce agricultural output used in production of food services. However, the expansion of cropland and accumulated GHG emissions from land use change appear relatively small. Decline in crop yields also depresses demand for processed food

services, whereas the production of biofuels remains practically unchanged.

We then contrast this optimal path to that obtained when the uncertainty is not ignored, thereby demonstrating the implications of factoring this in at the optimization stage.

Bateman, I., Mace, G., Fezzi, C., Atkinson, G. and Turner, K.: 2011, Economic Analysis for Ecosystem Service Assessments, *Environmental and Resource Economics* **48**(2), 177–218.

Bellman, R.: 1957, *Dynamic Programming*, Princeton University Press.

Benayas, J., Newton, A., Diaz, A. and Bullock, J.: 2009, Enhancement of Biodiversity and Ecosystem Services by Ecological Restoration: a Meta-analysis, *Science* **325**(5944), 1121–1124.

Bentsen, M., Bethke, I., Debernard, J., Iversen, T., Kirkevåg, A., Seland, Ø., Drange, H., Roelandt, C., Seierstad, I., Hoose, C. et al.: 2012, The Norwegian Earth System Model, NorESM1-M-Part 1: Description and Basic Evaluation, *Geoscientific Model Development Discussions* **5**, 2843–2931.

Cai, Y.: 2010, *Dynamic Programming and its Application in Economics and Finance*, PhD thesis, Stanford University.

Cai, Y. and Judd, K. L.: 2010, Stable and Efficient Computational Methods for Dynamic Programming, *Journal of the European Economic Association* **8**(2-3), 626–634.

Cai, Y. and Judd, K. L.: 2012a, Dynamic Programming with Hermite approximation, *Working Paper 18540*, National Bureau of Economic Research.

Cai, Y. and Judd, K. L.: 2012b, Dynamic Programming with Shape-preserving Rational Spline Hermite Interpolation, *Economics Letters* **117**(1), 161–164.

Cai, Y. and Judd, K. L.: 2012c, Shape-preserving Dynamic Programming, *Mathematical Methods of Operations Research* **forthcoming**.

Cai, Y. and Judd, K. L.: 2013, Advances in Numerical Dynamic Programming and New Applications, *in* K. L. Judd and K. Schmedders (eds), *Handbook of Computational Economics*, Elsevier.

Cai, Y., Judd, K. L., Thain, G. and Wright, S. J.: 2013, Solving Dynamic Programming Problems on a Computational Grid, *Working Paper 18714*, National Bureau of Economic Research.

Cassman, K. G.: 1999, Ecological Intensification of Cereal Production Systems: Yield Potential, Soil Quality, and Precision Agriculture, *Proceedings of the National Academy of Sciences* **96**(11), 5952–5959.

Cassman, K., Grassini, P. and van Wart, J.: 2010, Crop Yield Potential, Yield Trends, and Global Food Security in a Changing Climate, *in* D. Hillel and C. Rosenzweig (eds), *Handbook of Climate Change and Agroecosystems*, Imperial College Press, pp. 37–51.

Chakravorty, U., Hubert, M., Moreaux, M. and Nostbakken, L.: 2011, Will Biofuel Mandates Raise Food Prices?, *Working Paper 2011-01*, Department of Economics, University of Alberta.

Chazdon, R.: 2008, Beyond Deforestation: Restoring Forests and Ecosystem Services on Degraded Lands, *Science* **320**(5882), 1458–1460.

Collins, W., Bellouin, N., Doutriaux-Boucher, M., Gedney, N., Hinton, T., Jones, C., Liddicoat, S., Martin, G. et al.: 2008, Evaluation of the HadGEM2 Model, *Hadley Center Tech. Note* **74**.

Costanza, R., d'Arge, R., De Groot, R., Farber, S., Grasso, M., Hannon, B., Limburg, K., Naeem, S., O'Neill, R., Paruelo, J. et al.: 1997, The Value of the World's Ecosystem Services and Natural Capital, *Nature* **387**(6630), 253–260.

Cranfield, J., Eales, J., Hertel, T. and Preckel, P.: 2003, Model Selection when Estimating and Predicting Consumer Demands using International, Cross Section Data, *Empirical Economics* **28**(2), 353–364.

Daily, G.: 1997, *Nature's Services: Societal Dependence on Natural Ecosystems*, Island Pr.

Deaton, A. and Muellbauer, J.: 1980, An Almost Ideal Demand System, *The American Economic Review* **70**(3), 312–326.

Dufresne, J.-L., Foujols, M.-A., Denvil, S., Caubel, A., Marti, O., Aumont, O., Balkanski, Y., Bekki, S., Bellenger, H., Benshila, R. et al.: 2012, Climate Change Projections using the IPSL-CM5 Earth System Model: from CMIP3 to CMIP5, *Climate Dynamics* pp. 1–43.

Dunn, J., Eason, J. and Wang, M.: 2011, Updated Sugarcane and Switchgrass Parameters in the GREET Model, *Technical report*, Center for Transportation Research, Argonne National Laboratory.

Dunne, J. P., John, J. G., Shevliakova, E., Stouffer, R. J., Krasting, J. P., Malyshev, S. L., Milly, P., Sentman, L. T., Adcroft, A. J., Cooke, W. et al.: 2013, GFDL's ESM2 Global Coupled Climate?Carbon Earth System Models. Part II: Carbon System Formulation and Baseline Simulation Characteristics, *Journal of Climate* **26**(7), 2247–2267.

Evans, L. and Fischer, R.: 1999, Yield Potential: its Definition, Measurement, and Significance, *Crop Science* **39**(6), 1544–1551.

Fearnside, P.: 2000, Global Warming and Tropical Land-use Change: Greenhouse Gas Emissions from Biomass Burning, Decomposition and Soils in Forest Conversion, Shifting Cultivation and Secondary Vegetation, *Climatic Change* **46**(1), 115–158.

Geroski, P.: 2000, Models of Technology Diffusion, *Research Policy* **29**(4-5), 603–625.

Gill, P., Murray, W., Saunders, M. and Wright, M.: 1998, Users Manual for NPSOL 5.0, A FORTRAN Package for Nonlinear Programming, *Technical Report SOL 86-1*, Department of Operations Research, Stanford University.

Golub, A., Hertel, T. and Sohngen, B.: 2009, Land Use Modeling in Recursively-Dynamic GTAP Framework, *in* T. Hertel, S. Rose and R. Tol (eds), *Economic Analysis of Land Use in Global Climate Change Policy*, Routledge, pp. 235–278.

Gumpenberger, M., Vohland, K., Heyder, U., Poulter, B., Macey, K., Rammig, A., Popp, A. and Cramer, W.: 2010, Predicting Pan-Tropical Climate Change Induced Forest Stock Gains and Losses: Implications for REDD, *Environmental Research Letters* **5**(1), 014013.

Gurgel, A., Reilly, J. and Paltsev, S.: 2007, Potential Land Use Implications of a Global Biofuels Industry, *Journal of Agricultural & Food Industrial Organization* **5**(2), 1–34.

Hanoch, G.: 1975, Production and Demand Models with Direct or Indirect Implicit Additivity, *Econometrica* **43**(3), 395–419.

Hertel, T. W., Burke, M. B. and Lobell, D. B.: 2010, The Poverty Implications of Climate-Induced Crop Yield Changes by 2030, *Global Environmental Change* **20**(4), 577–585.

Hocking, M., Stolton, S. and Dudley, N.: 2000, *Evaluating Effectiveness: A Framework for Assessing the Management of Protected Areas*, IUCN, Gland, Switzerland, and Cambridge, UK.

Houghton, R.: 2003, Revised Estimates of the Annual Net Flux of Carbon to the Atmosphere from Changes in Land Use and Land Management 1850–2000, *Tellus B* **55**(2), 378–390.

Jones, J. W., Hoogenboom, G., Porter, C., Boote, K., Batchelor, W., Hunt, L., Wilkens, P., Singh, U., Gijsman, A. and Ritchie, J.: 2003, The DSSAT Cropping System Model, *European Journal of Agronomy* **18**(3), 235–265.

Judd, K. L.: 1998, *Numerical Methods in Economics*, The MIT press.

Lobell, D. B. and Burke, M. B.: 2008, Why are Agricultural Impacts of Climate Change so Uncertain? The Importance of Temperature Relative to Precipitation, *Environmental Research Letters* **3**(3), 034007.

Lobell, D. B., Cassman, K. G. and Field, C. B.: 2009, Crop Yield Gaps: their Importance, Magnitudes, and Causes, *Annual Review of Environment and Resources* **34**(1), 179.

Lobell, D. B. and Field, C. B.: 2007, Global Scale Climate - Crop Yield Relationships and the Impacts of Recent Warming, *Environmental Research Letters* **2**(1), 014002.

Lobell, D., Schlenker, W. and Costa-Roberts, J.: 2011, Climate Trends and Global Crop Production Since 1980, *Science* **333**(6042), 616–620.

Long, S.: 1991, Modification of the Response of Photosynthetic Productivity to Rising Temperature by Atmospheric CO2 Concentrations: Has its Importance been Underestimated?, *Plant, Cell & Environment* **14**(8), 729–739.

Long, S. P., Ainsworth, E. A., Leakey, A. D., Nösberger, J. and Ort, D. R.: 2006, Food for Thought: Lower-Than-Expected Crop Yield Stimulation with Rising CO2 Concentrations, *Science* **312**(5782), 1918–1921.

McFarland, J., Reilly, J. and Herzog, H.: 2004, Representing Energy Technologies in Top-down Economic Models Using Bottom-up Information, *Energy Economics* **26**, 685–707.

Meyer, S., Binfield, J., Westhoff, P. and Thompson, W.: 2011, U.S. Biofuels Baseline: The Impact of Extending the $0.45 Ethanol Blenders Credit, *FAPRI-MU Report 07-11*, Food and Agricultural Policy Research Institute at the University of Missouri-Columbia.

Moss, R. H., Babiker, M., Brinkman, S., Calvo, E., Carter, T., Edmonds, J. A., Elgizouli, I., Emori, S., Lin, E., Hibbard, K. et al.: 2008, Towards New Scenarios for Analysis of Emissions, Climate Change, Impacts, and Response Strategies, *Technical Report PNNL-SA-63186*, Pacific Northwest National Laboratory (PNNL), Richland, WA (US).

National Research Council: 2005, *Valuing Ecosysten Services: Toward Better Eenvironmental Ddecision-Making*, National Academies Press.

National Research Council: 2011, *Renewable Fuel Standard: Potential Economic and Environmental Effects of U.S. Biofuel Policy*, National Academies Press.

Nesshöver, C., Aronson, J., Blignaut, J., Lehr, D., Vakrou, A. and Wittmer, H.: 2009, Investing in Ecological Infrastructure, *in* P. ten Brink (ed.), *The Economics of Ecosystems and Biodiversity: National and International Policy Making. An Output of TEEB*, Earthscan, pp. 401–448.

Paltsev, S., Reilly, J., Jacoby, H., Eckaus, R., McFarland, J., Sarofim, M., Asadoorian, M. and Babiker, M.: 2005, The MIT Emissions Prediction and Policy Analysis (EPPA) Model: Version 4, *Technical report*, MIT Joint Program on the Science and Policy of Global Change.

Parry, M. L., Rosenzweig, C., Iglesias, A., Livermore, M. and Fischer, G.: 2004, Effects of Climate Change on Global Food Production under SRES Emissions and Socio-Economic Scenarios, *Global Environmental Change* **14**(1), 53–67.

Popp, A., Dietrich, J., Lotze-Campen, H., Klein, D., Bauer, N., Krause, M., Beringer, T., Gerten, D. and Edenhofer, O.: 2011, The Economic Potential of Bioenergy for Climate Change Mitigation with Special Attention Given to Implications for the Land System, *Environmental Research Letters* **6**(3).

Reilly, J., Paltsev, S., Felzer, B., Wang, X., Kicklighter, D., Melillo, J., Prinn, R., Sarofim, M., Sokolov, A. and Wang, C.: 2007, Global Economic Effects of Changes in Crops, Pasture, and Forests due to Changing Climate, Carbon Dioxide, and Ozone, *Energy Policy* **35**(11), 5370–5383.

Rimmer, M. and Powell, A.: 1996, An Implicitly Additive Demand System, *Applied Economics* **28**(12), 1613–1622.

Rosenzweig, C., Elliott, J., Deryng, D., Ruane, A., Arneth, A., Bootef, K., Folberth, C., Glotter, M., Khabarov, N., Müller, C., Neumann, K., Piontek, F., Pugh, T., Schmid, E., Stehfest, E. and Jones, J.: 2013, Assessing Agricultural Risks of Climate Change in the 21st Century in a Global Gridded Crop Model Intercomparison, *Proceedings of the National Academy of Sciences* **in press**.

Rust, J.: 2008, *Dynamic Programming*, The New Palgrave Dictionary of Economics, London, UK, Palgrave Macmillan, Ltd.

Sorrell, S. and Dimitropoulos, J.: 2008, The Rebound Effect: Microeconomic Definitions, Limitations and Extensions, *Ecological Economics* **65**(3), 636–649.

Steinbuks, J. and Hertel, T.: 2012, Forest, Agriculture, and Biofuels in a Land use model with Environmental services (FABLE), *GTAP Working Paper 71*, Center for Global Trade Analysis, Department of Agricultural Economics, Purdue University.

van Meijl, H. and van Tongeren, F.: 1999, Endogenous International Technology Spillovers and Biased Technical Change in the GTAP Model, *GTAP Technical Paper 15*, Center for Global Trade Analysis, Purdue University.

Watanabe, S., Hajima, T., Sudo, K., Nagashima, T., Takemura, T., Okajima, H., Nozawa, T., Kawase, H., Abe, M., Yokohata, T. et al.: 2011, MIROC-ESM 2010: Model Description and Basic Results of CMIP5-20c3m Experiments, *Geoscientific Model Development* **4**, 845–872.

Yu, W., Hertel, T., Preckel, P. and Eales, J.: 2004, Projecting World Food Demand Using Alternative Demand Systems, *Economic Modelling* **21**(1), 99–129.